Journal of Power Sources 184 (2008) 325–330

Contents lists available at ScienceDirect

Journal of Power Sources

journal homepage: www.elsevier.com/locate/jpowsour

A doubly-fed induction generator-based wind generation system with quasi-sine rotor injection

S. Yuvarajan*, Lingling Fan

Electrical and Computer Engineering Department, North Dakota State University, Fargo, ND 58105, United States

ARTICLE INFO

Article history:
Received 25 March 2008
Received in revised form 27 May 2008
Accepted 29 May 2008
Available online 3 June 2008

Keywords:
Doubly-fed induction generator (DFIG)
Wind generation
Quasi-sine wave
Rotor injection
Total harmonic distortion (THD)

ABSTRACT

Wind generating systems use doubly-fed induction generators (DFIGs) to achieve high conversion efficiency and to reduce the installation cost. The paper proposes and analyzes a simple DFIG-based wind generation system in which the excitation power is obtained from a photovoltaic (PV) panel and battery. The proposed scheme is suitable for small wind power systems for which a complex field orientation control is not justified. It can be used for stand-alone operation and also grid-tied operation. The rotor of the DFIG is applied with a quasi-sine wave instead of a sine wave. The operation and harmonic characteristics of the scheme are established using analysis, simulation, and experimentation. The details of the control circuit are given along with the experimental waveforms of voltages and currents and frequency spectra. The total harmonic distortion in the output current is found to be around 8%.

1. Introduction

Doubly-fed induction generators (DFIGs) are increasingly used in efficient wind generating systems which allow variable-speed operation. These systems use a wound-rotor induction machine to convert the mechanical power from the wind turbine into a fixed-frequency ac output, with a fraction of the output coming from rotor injection. Normally a double converter supplies the rotor with a sinusoidal current whose frequency depends on the speed of the rotor or the wind turbine. The double converter allows power flow in both directions depending on the speed which could be below synchronous speed or above synchronous speed. It handles a maximum of 25% of the stator output power for a speed variation of ±33% about synchronous speed for normal values of slip [1,2]. Thus the system uses power converters as well as filters with correspondingly lower ratings. The converters and control scheme proposed allow independent active and reactive power control based on field orientation which is very complex and justifies its use for large wind generating systems.

With the new concept of micro-grids, smaller wind generating systems are proposed and their output is either fed to the grid or put to stand-alone use. Such systems need simple converters and control schemes. Moreover, the availability of other renewable energy sources like PV power can be exploited in providing the excitation power in the case of a doubly fed induction generator. The paper analyzes the performance of a DFIG whose rotor is fed with a three-level quasi-sine wave generated from a simple bridge inverter. The dc input to the inverter is from a group of PV panels and a maximum power point tracking (MPPT) converter. The output from the PV panels is buffered through a set of batteries which absorb the excess power from the PV panels, or from the rotor when the speed goes above the synchronous speed of the DFIG. In the latter case, the power converter operates as a rectifier.

A 5 HP wound-rotor induction motor is used in the analysis and experimentation. The performance is studied when the rotor injection voltage is a three-level quasi-sine wave and both simulated and experimental waveforms are given. The quasi-sine wave is obtained using a six pulse, three-phase bridge inverter and a very simple control circuit. A harmonic analysis of the stator current/voltage waveform shows that the total harmonic distortion (THD) is low. The performance characteristics of the machine with quasi-sine-wave injection are obtained in terms of the harmonics present in the stator and their amplitudes.

2. Variable-speed DFIG system

The block diagram of a conventional wind generating system with a DFIG and dual power converters is shown in Fig. 1. The stator of the DFIG or wound-rotor induction machine is connected to the grid. The rotor is driven by the wind generator whose pitch angle is adjusted for optimum performance resulting in a variable-speed operation. The rotor terminals are applied with an ac voltage

* Corresponding author. Tel.: +1 701 231 7365; fax: +1 701 231 8677.
E-mail address: Subbaraya.yuvarajan@ndsu.edu (S. Yuvarajan).

0378-7753/$ – see front matter
doi:10.1016/j.jpowsour.2008.05.076

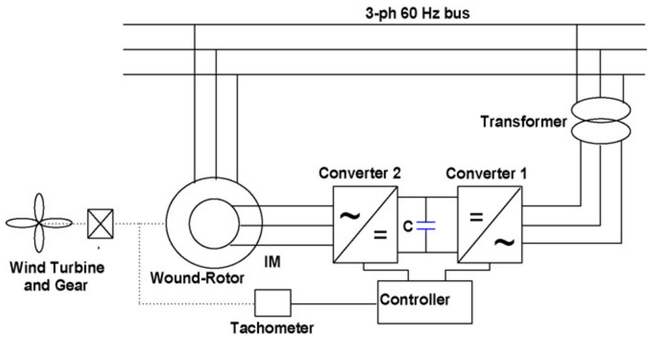

Fig. 1. Block diagram of conventional wind generator with a DFIG.

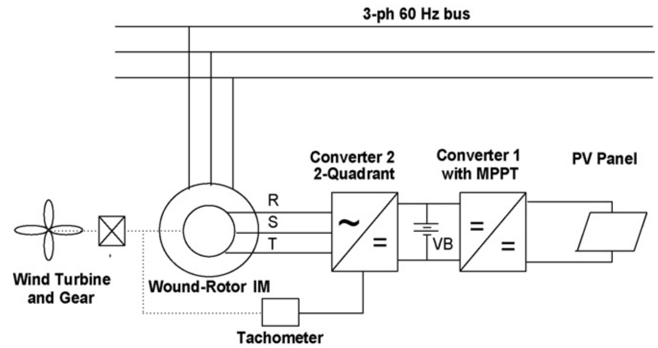

Fig. 2. Block diagram of proposed system.

of a desired frequency and amplitude. When the machine is driven below synchronous speed, the output power from the stator is equal to the sum of the mechanical power from the wind turbine and the ac power injected into the rotor. In this case, Converter 1 works as a rectifier and Converter 2 works as an inverter. When the machine is driven above synchronous speed, power is recovered form the rotor with Converter 2 working as a rectifier and Converter 1 working as an inverter. Control schemes include reactive and active power control through the two rotor side converters [3] and it is implemented using a digital signal processor (DSP).

The stator frequency f_s is kept constant at 60 Hz irrespective of the rotor speed. If the machine has P poles and the rotor speed is N rpm, then the frequency of the rotor voltage to be injected is given by

$$f_r = f_s - f_m \quad (1)$$

where $f_m = PN/120$ Hz. A tachogenerator is used to sense the speed of the rotor and suitably adjust the injection frequency. The power relation is given by

$$P_r = sP_s \quad (2)$$

where the slip is given by $s = (N_s - N)/N_s$.

3. Operation of the proposed system

The block diagram of the proposed system is shown in Fig. 2. As in the conventional variable-speed scheme, the stator may be connected to the 60 Hz bus, or it can supply an isolated load. The wind turbine supplies most of the power (mechanical) to the DFIG and the balance comes from rotor injection. The output from the PV panel is supplied to the rotor after it is converted to a dc voltage of suitable amplitude using Converter 1 and then to an ac using a three-phase bridge inverter (Converter 2). The dc–dc converter

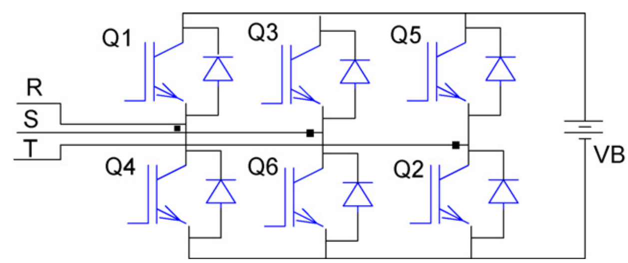

Fig. 3. Power circuit of three-phase bridge inverter.

(Converter 1) includes a simple maximum power point tracking (MPPT) scheme [4]. A battery V_B is included between the two converters and it helps in three different ways: (a) as a buffer storing the extra energy from the PV panel when the maximum power available is more than what is required for rotor injection, (b) as a dc source providing injection power to operate the wind energy system in the absence of sun light and (c) as a buffer storing the power recovered from the machine when the speed is higher than the synchronous speed.

The dc–dc converter is a standard buck-boost or Sepic that can provide enough voltage under widely varying light conditions. The inverter is a three-level three-phase bridge circuit with IGBTs, with reverse diodes across each as shown in Fig. 3. The gate signals to the IGBTs are generated by the circuit shown in Fig. 4 which consists of a 555 timer and a set of flip–flops connected as a ring counter. The frequency of the periodic pulses generated by the 555 timer should be $3f_r$ and it is varied by the control voltage V_c. The control circuit is simple and it does not need sine waves and triangular waves used in Sine PWM implementation. It is very easy to adjust the rotor injection frequency by simply varying V_c. The output line voltage of the inverter is a quasi-sine wave with levels 0, V_s, and $-V_s$ where

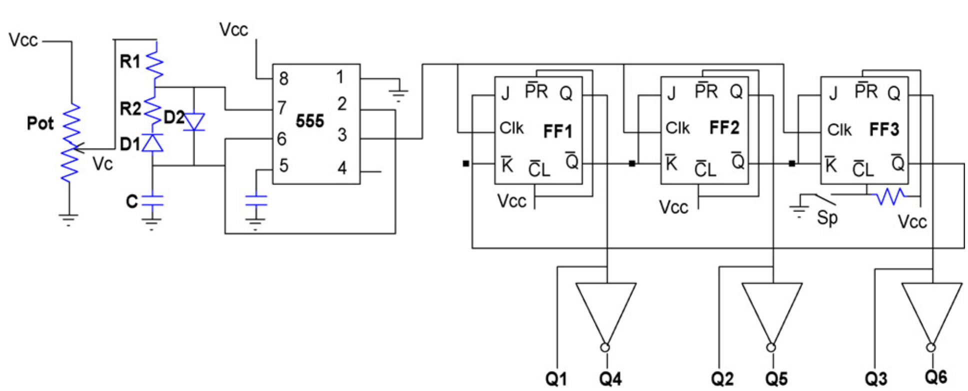

Fig. 4. Circuit diagram of gate signal generator for the proposed system.

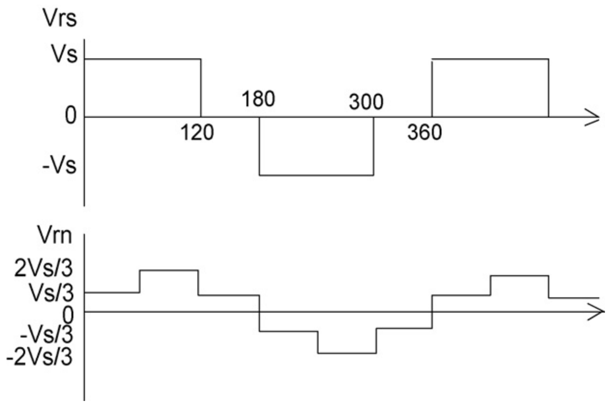

Fig. 5. Quasi-sine waveforms of line and phase voltage applied to the rotor.

V_s is the dc link voltage supplied to the inverter and one of the three line voltages and a phase voltage are shown in Fig. 5. A harmonic analysis of the phase voltage waveform gives the rms value of the nth harmonic as

$$V_{n,\text{rms}} = \frac{\sqrt{2}}{n\pi} V_s \sin 60^\circ = \frac{0.78 V_s}{n} \tag{3}$$

where $n = 6k \pm 1$ and $k = 0, 1, 2, 3, \ldots$.

The three-phase voltage of Fig. 5 is applied to the rotor terminals R, S, T of the DFIG shown in Fig. 2. The induction machine has a set of leakage and mutual inductances as shown in the per-phase equivalent circuit of Fig. 6. These inductors help to attenuate the harmonics in the voltage induced in the stator. There is a two-step attenuation of the harmonics, first in the current injected into the rotor and then the voltage induced in the stator. The resulting output voltage from the stator has a small harmonic distortion and the output voltage approximates a 60 Hz sine wave. The output voltage can be either fed to the grid, or it can be fed to a load which is an advantage not available in the conventional scheme of Fig. 1.

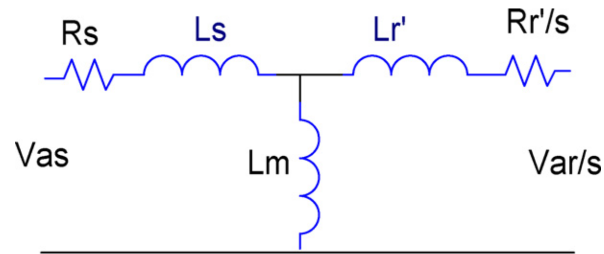

Fig. 6. Equivalent circuit of induction machine.

The output voltage from the stator contains harmonics which result from the harmonics present in the rotor-injected voltage ($(6k \pm 1)f_r$) and the mechanical frequency (f_m). Thus the stator will have the following harmonics: $5f_r - f_m$, $7f_r + f_m$, $11f_r - f_m$, $13f_r + f_m$, ... The lowest order harmonic (LOH) is $5f_r - f_m$. It is desirable to have a higher LOH which is possible for lower values of f_m or for lower speeds. This fact may be used in designing the gear ratio for the wind turbine. For each harmonic voltage applied to the rotor, the harmonic current can be calculated by using the equivalent circuit of Fig. 6 and the voltage from Eq. (3).

4. Simulation of the proposed system

The DFIG system is simulated using PSIM [5] which has models of DFIG, IGBTs, and dc and ac sources. The simulation diagram is shown in Fig. 7. The parameters of the wound-rotor induction machine used in the simulation and the experimentation are given in Table 1. The input to the bridge inverter is a dc voltage obtained from a set of PV panels and a dc–dc converter which includes an MPPT section. The DFIG is driven by a separately excited dc motor which represents the wind turbine. The speed of the DFIG can be

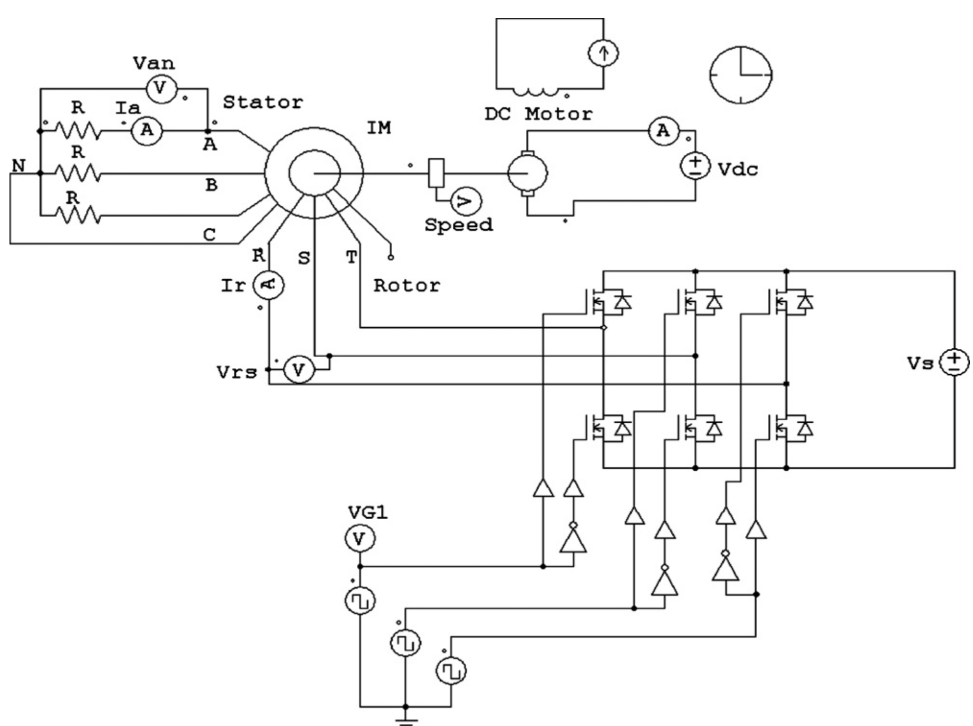

Fig. 7. PSIM simulation diagram of proposed DFIG system.

Table 1
DFIG parameters

R_s (Ω)	0.32
L_s (mH)	1.19
R_r (Ω)	0.36
L_r (mH)	1.34
L_m (mH)	39.46

varied by varying the armature voltage applied to the dc motor. The simulation is run for a sufficiently long time so the system reaches a steady speed. For a given rotor speed, the frequency of the inverter is adjusted so that the stator frequency is 61 Hz. The simulation waveforms of the voltage applied to the rotor, rotor current, and stator current are given in Fig. 8 and the frequency spectra are shown in Fig. 9. The following are the parameters and frequencies used in the analysis, simulation, and experiment:

Motor speed $N_m = 1108$ rpm ($f_m = 37$ Hz).
Rotor frequency (f_r) = 24 Hz.
Stator frequency (f_s) = 61 Hz.
dc voltage to inverter (V_s) = 30 V.
Stator load (R) = 22 Ω per phase; Wye-connected.

It is seen that the rotor voltage contains considerable amount of harmonics whereas the rotor and stator currents have lower and much lower harmonics, respectively. Table 2 includes the different harmonics and their amplitudes present in the stator current.

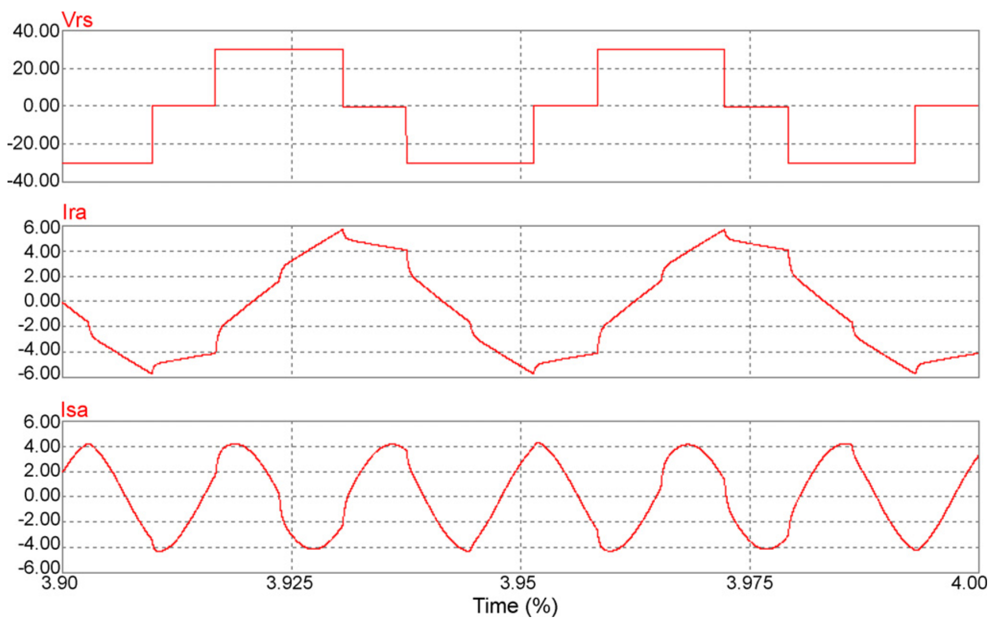

Fig. 8. Simulation waveforms of rotor voltage, rotor current, and stator current.

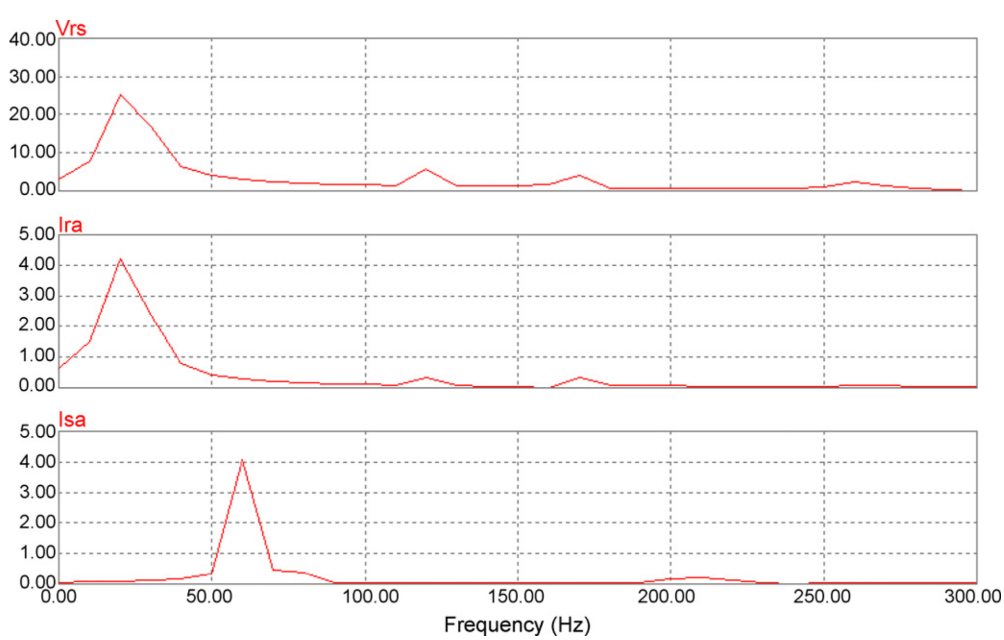

Fig. 9. Frequency spectrum of the waveforms in Fig. 8.

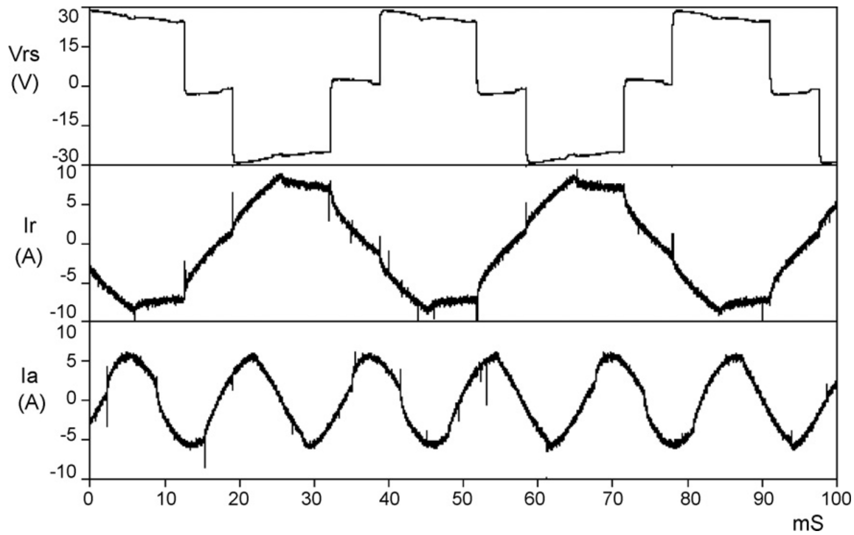

Fig. 10. Experimental waveforms of rotor voltage, rotor current, and stator current.

Table 2
Harmonics in stator current

Frequency components	% amplitude in stator current		
	Analysis	Simulation	Experiment
61	100	100	100
83	5.49	5.00	4.57
205	6.42	6.00	3.36
227	2.87	2.92	2.31
349	3.04	2.14	1.64
THD	9.63	8.61	6.29

The total harmonic distortion is computed as 8.61%. The analytically calculated values of harmonics and THD are also given for comparison.

The closed loop implementation is simple. The output of the speed transducer is used to control the frequency of the voltage to be injected into the rotor. It is also used to vary the dc link voltage applied to the inverter which controls the amplitude of the stator output voltage and maintains it at a desired level.

5. Experimental results

The 5 HP wound rotor whose parameters are given in Table 1 was driven by a dc motor. The IGBTs in the three-step inverter shown in Fig. 3 were supplied with gate pulses generated by the control circuit of Fig. 4. The dc link voltage to the bridge inverter was manually varied. For a given motor speed, the frequency of rotor injection was adjusted to give a stator frequency of 61 Hz. The stator output was supplied to a three-phase resistive load. The waveforms of the voltage applied to the rotor and the resulting currents in the rotor and the stator were recorded using a digital storage oscilloscope and shown in Fig. 10. The frequency spectra of the rotor voltage, rotor current, and stator current obtained using a post-processing software are given in Fig. 11. The software is also used to compute the harmonics and the THD in the stator current which are included in Table 2. The THD is measured as 6.29% which is lower than the value obtained using simulation and mathematical analysis.

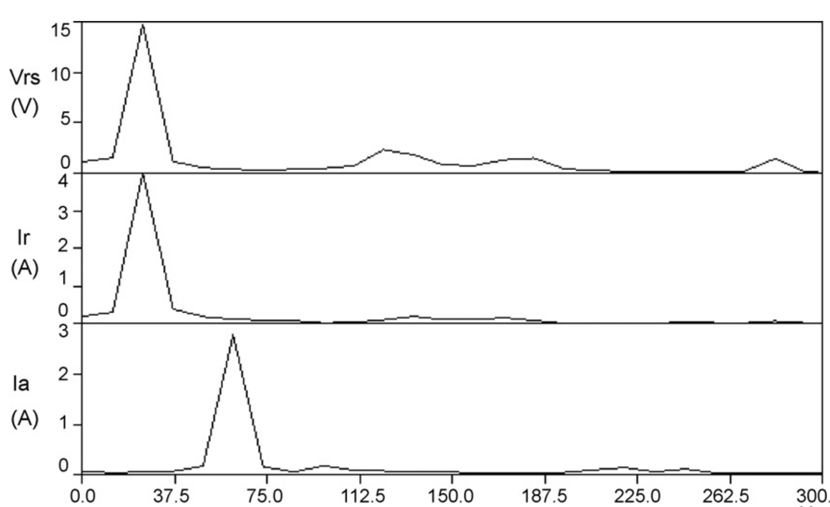

Fig. 11. Frequency spectrum of the waveforms in Fig. 10.

6. Conclusions

A simple and economical power conversion scheme for a DFIG-based wind generation system is proposed. The scheme allows the use of PV power to provide rotor injection for the DFIG. The output sine wave from the stator has low harmonics and can be used for grid-tied operation as well as stand-alone operation. The details of the control circuit are presented. The experimental results from a prototype wind generation system are presented along with the results from simulation and analysis.

References

[1] S. Muller, M. Deicke, R.W. De Doncker, IEEE Industry Applications Magazine (May–June) (2002) 26–33.
[2] A. Petersson, L. Harnefors, T. Thiringer, IEEE Transactions on Power Electronics 20 (January (1)) (2005) 227–235.
[3] Y. Tang, L. Xu, IEEE Transactions on Power Electronics 10 (July (4)) (1995) 472–478.
[4] S. Yuvarajan, D. Yu, S. Xu, Journal of Power Sources 135 (September (1–2)) (2004) 327–331.
[5] PSIM, A software by Powersim Technologies, Professional Version 6.05, 2004.